Hairy Reissner-Nordström black holes with asymmetric vacua

Xiao Yan Chew[1,*] and Dong-han Yeom[2,3,4,†]

[1]*School of Science, Jiangsu University of Science and Technology, 212100 Zhenjiang, China*
[2]*Department of Physics Education, Pusan National University, Busan 46241, Republic of Korea*
[3]*Research Center for Dielectric and Advanced Matter Physics, Pusan National University, Busan 46241, Republic of Korea*
[4]*Leung Center for Cosmology and Particle Astrophysics, National Taiwan University, Taipei 10617, Taiwan*

(Received 28 January 2024; accepted 18 July 2024; published 15 August 2024)

We minimally coupled a scalar potential $V(\phi)$ with asymmetric vacua to the Einstein gravity to numerically construct the hairy Reissner-Nordström black hole (RNBH) as a direct generalization of RNBHs to possess scalar hair. By fixing the electric charge to mass ratio q, a branch of hairy RNBHs bifurcates from the RNBH when the scalar field ϕ_H is nontrivial at the horizon. The values of q are bounded for $0 \leq q \leq 1$, which contrast to a class of hairy black holes with $q > 1$ in the Einstein-Maxwell-scalar theory. We find that the profiles of solutions affected by the competition between the strength of ϕ_H and q, for instance, the gradient of scalar field at the horizon can increase very sharply when $q \to 1$ and ϕ_H is small, but its gradient can be very small which is independent of q when ϕ_H is large. Furthermore, the weak energy condition of hairy RNBHs, particularly at the horizon can be satisfied when $q > 0$.

DOI: 10.1103/PhysRevD.110.044036

I. INTRODUCTION

According to the no-hair theorem [1–3], the state of black holes in general relativity (GR) can only be described by the three global charges which are the mass, electrical charge, and angular momentum. The Reissner-Nordström black hole (RNBH) [4,5] is the solution to the Einstein-Maxwell theory and satisfies the no-hair theorem. Nevertheless, a black hole is known as a hairy black hole when it is supported by a matter field outside the event horizon and may possess additional global charge (refers to "hair") which is associated with the matter field. Hairy black holes can exhibit a deviation of their properties from the electrovacuum black holes in the strong gravity regime but are indistinguishable in the weak gravity regime. A mechanism which is known as the spontaneous scalarization (SS) to allow black holes can evade the no-hair theorem to possess a nontrivial scalar field ϕ outside the horizon; hence the RN black hole can be extended to a broader class of charged hairy black holes; for instance, a various form of scalar function $f(\phi)$ nonminimally couples with the Maxwell field [6–32] in the Einstein-Maxwell-scalar theory can give rise to the tachyonic instabilities so that charged hairy black holes can be spontaneously scalarized from the RNBH. A few decades ago T. Damour and G. Esposito-Farèse [33] proposed the concept of SS to predict the deviation of properties for the neutron stars from GR in the strong gravity regime, but it becomes indistinguishable in the weak gravity regime within the framework of the scalar-tensor theory, which nonminimally couples a scalar function with the Ricci scalar.

However, one may overlook that an RNBH can also be extended to another class of charged hairy black holes in the simplest and direct manner, i.e., one can minimally couple the Einstein gravity and Maxwell field with a scalar potential $V(\phi)$. By properly introducing the form of $V(\phi)$ which is associated with the profile of $V(\phi)$ to evade the no-hair theorem, the solutions of hairy black holes can be bifurcated from the electrovacuum black holes, and they are regular everywhere in the spacetime. Recently, the authors have employed two different profiles of $V(\phi)$ to construct the neutral hairy black holes without the anticipation of other extended objects, for instance the Gauss-Bonnet term or matter fields and study their properties in detail [34–36]. The first profile of $V(\phi)$ with the shape of two asymmetric vacua which contain a local maximum, a local minimum, and a global minimum to describe the phase transition of vacuum bubbles from the false vacuum (local minimum) to the true vacuum (global minimum) [37]. The second profile of $V(\phi)$ with the shape of the inverted Mexican hat contains two degenerate maxima and a local minimum [36]. Therefore, we generalize those neutral hairy black holes in [35] to possess an electric charge and study their

*Contact author: xiao.yan.chew@just.edu.cn
†Contact author: innocent.yeom@gmail.com

properties in this paper. Other choices of $V(\phi)$ or a similar construction can refer to [38–46].

On the other hand, the RNBH possesses an inner horizon, instead of the outer horizon. The inner horizon is known as the Cauchy horizon which can preserve the predictability in GR. Recently, various attempts have been made to prove the nonexistence of a Cauchy horizon for the static and charged black holes [47–51]. For instance, the investigations for the interior of the static charged hairy black holes with spherical and planar symmetries in the Born-Infield theory [47] and the Einstein-Maxwell-Klein-Gordon theory with a scalar potential of a complex scalar field [48] have been done numerically to demonstrate the nonexistence of the Cauchy horizon. However, the interior of the charged black holes will not remain as the static case when we consider the scenario of gravitational collapse with the time evolution. Thus, the authors (we) [50] adopted the double-null formalism to investigate the gravitational collapse of charged black holes and found that the behavior of the Cauchy horizon could behave differently from the static case; for instance, the Cauchy horizon cannot be generated during collapse of the charged black holes in the Brans-Dicke theory, which demonstrates that the scalar field at the outer horizon does not lead to the formation of the Cauchy horizon in the evolution. Therefore, it provides a good motivation for us to construct such charged black holes as a first step to studying the existence of the Cauchy horizon by any approach.

This paper is organized as follows. In Sec. II, we briefly introduce our theoretical setup comprising the Lagrangian and the metric ansatz. Then, we derive the set of coupled differential equations and study the asymptotic behavior of the functions. In Sec. II C, we briefly introduce the quantities of interest for the black holes. In Sec. II D, we perform a spherical perturbation to the background of hairy RNBHs and the matter fields to calculate numerically the (un)stable mode. In Sec. III, we present and discuss our numerical findings. Finally, in Sec. IV, we summarize our work and present an outlook.

II. THEORETICAL SETTING

A. Theory and *Ansätze*

In the Einstein-Maxwell-Klein-Gordon (EMKG) system, we consider an asymmetric potential $V(\phi)$ of a scalar field ϕ which is given by [34,35] to minimally couple with the Maxwell field and the Einstein gravity,

$$S = \int d^4x\sqrt{-g}\left[\frac{R}{16\pi G} - \frac{1}{4}F_{\mu\nu}F^{\mu\nu} - \frac{1}{2}\partial_\mu\phi\partial^\mu\phi - V(\phi)\right], \tag{1}$$

where $F_{\mu\nu} = \partial_\mu A_\nu - \partial_\nu A_\mu$ is the electromagnetic field strength tensor. The explicit form of $V(\phi)$ is given by

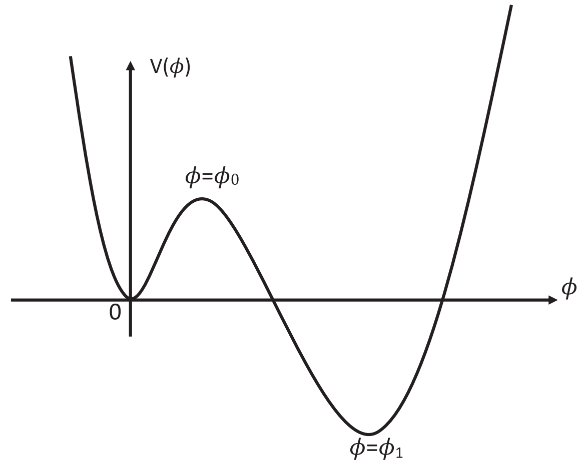

FIG. 1. The authors have considered the scalar potential $V(\phi)$ with a false vacuum at $\phi = 0$, a barrier at $\phi = \phi_0$, and a true vacuum at $\phi = \phi_1$ to construct the hairy black holes [35].

$$V(\phi) = \frac{V_0}{12}(\phi - a)^2[3(\phi - a)^2 - 4(\phi - a)(\phi_0 + \phi_1) + 6\phi_0\phi_1], \tag{2}$$

with a, V_0, ϕ_0, and ϕ_1 as the constants. As shown in Fig. 1, when $\phi = a$, this potential $V(\phi)$ possesses a local minimum which is also a zero of $V(\phi)$. The asymptotic value of ϕ at the infinity is fixed by $\phi = a$. $V(\phi)$ also possesses a local maximum at $\phi = a + \phi_0$ and a global minimum at $\phi = a + \phi_1$. In this paper, we choose $a = 0$ such that the scalar field is asymptotically flat at the spatial infinity. Note that the asymmetrical profile of $V(\phi)$ is caused by the appearance of cubic term ϕ^3; thus $V(\phi)$ can become symmetric if the cubic term disappears; for instance, the authors recently have employed a symmetric profile of $V(\phi)$ which possesses two degenerate global maxima and local minimum to construct the hairy black holes [36] and gravitating scalaron [52]. Furthermore, a similar form of Eq. (2) has been applied to construct the Fermionic star [53].

Then we obtain the Einstein equation, Klein-Gordon equation, and Maxwell equation by varying the action [Eq. (1)] with respect to the metric, scalar field, and Maxwell field, respectively:

$$R_{\mu\nu} - \frac{1}{2}g_{\mu\nu}R = \beta T_{\mu\nu}, \tag{3}$$

$$\nabla_\mu\nabla^\mu\phi = \frac{dV}{d\phi}, \tag{4}$$

$$\nabla_\mu F^{\mu\nu} = 0, \tag{5}$$

where $\beta = 8\pi G$ and the stress-energy tensor $T_{\mu\nu}$ is given by

$$T_{\mu\nu} = -g_{\mu\nu}\left(\frac{1}{2}\partial_\alpha\phi\partial^\alpha\phi + V(\phi)\right) + \partial_\mu\phi\partial_\nu\phi + g^{\alpha\beta}F_{\mu\alpha}F_{\nu\beta} - \frac{1}{4}g_{\mu\nu}F_{\alpha\beta}F^{\alpha\beta}. \tag{6}$$

We employ the following spherically symmetric *Ansatz* to construct the charged hairy black hole solutions,

$$ds^2 = -N(r)e^{-2\sigma(r)}dt^2 + \frac{dr^2}{N(r)} + r^2(d\theta^2 + \sin^2\theta d\varphi^2), \tag{7}$$

where $N(r) = 1–2m(r)/r$ with $m(r)$ is the Misner-Sharp mass function [54]. Note that we can read off the mass of black holes with the condition $m(\infty) = M$ where M is the Arnowitt-Deser-Misner (ADM) mass. Moreover, the *Ansatz* for the gauge field is chosen to be

$$A_\mu = U(r)dt. \tag{8}$$

B. Ordinary differential equations (ODEs)

To derive the ordinary differential equations (ODEs) from Eqs. (3)–(5), we begin with Eq. (5) to directly obtain a first-order ODE,

$$U' = \frac{Qe^{-\sigma}}{r^2}, \tag{9}$$

where the prime denotes the derivative of the functions with respect to the radial coordinate r and we denote Q as the electric charge. The substitution of Eq. (7) into the EMKG system yields a set of nonlinear ODEs for the following functions:

$$m' = \frac{\beta}{4}r^2\left(N\phi'^2 + 2V + \frac{Q^2}{r^4}\right), \qquad \sigma' = -\frac{\beta}{2}r\phi'^2,$$
$$(e^{-\sigma}r^2N\phi')' = e^{-\sigma}r^2\frac{dV}{d\phi}. \tag{10}$$

If the scalar field vanishes ($\phi = 0$), then the trivial solution for the EMKG system is the RNBH which is given by

$$m(r) = M - \frac{Q^2}{2r}, \quad \sigma(r) = 0, \quad U(r) = U_\infty - \frac{Q}{r}, \tag{11}$$

where M is the ADM mass and U_∞ is the electric potential. The horizon r_H of the RNBH is given by $r_H = M + \sqrt{M^2 - Q^2}$. However, if the scalar field does not vanish, but the scalar potential vanishes ($V(\phi) = 0$), the solution of the above EMKG system is still the RNBH but with the scalar field diverging at the horizon. Hence, the proper introduction of $V(\phi)$ is very crucial so that it can regularize the scalar field at the horizon. Previously the authors considered Eq. (2) to construct the neutral hairy black holes and study their properties. Thus, in this paper, we generalize them to possess the electric charge Q.

To construct the charged hairy black hole solutions that are globally regular, the functions and their derivatives are required to be finite, particularly at the horizon. Hence, the asymptotic behavior of the functions at the horizon can be described by the power series expansions in which the few leading terms in the series expansion are given by

$$m(r) = \frac{r_H}{2} + m_1(r - r_H) + O((r - r_H)^2), \tag{12}$$

$$\sigma(r) = \sigma_H + \sigma_1(r - r_H) + O((r - r_H)^2), \tag{13}$$

$$\phi(r) = \phi_H + \phi_{H,1}(r - r_H) + O((r - r_H)^2), \tag{14}$$

$$U(r) = \frac{Qe^{-\sigma_H}}{r_H^2}(r - r_H) - \frac{Qe^{-\sigma_H}(2 + \sigma_1 r_H)}{2r_H^3}(r - r_H)^2 + O((r - r_H)^3), \tag{15}$$

where

$$m_1 = \frac{\beta}{4}r_H^2\left(2V(\phi_H) + \frac{Q^2}{r_H^4}\right), \qquad \sigma_1 = -\frac{\beta r_H}{2}\phi_{H,1}^2,$$
$$\phi_{H,1} = \frac{r_H\frac{dV(\phi_H)}{d\phi}}{1 - \beta r_H^2 V(\phi_H) - \frac{\beta Q^2}{2r_H^2}}. \tag{16}$$

Here σ_H and ϕ_H are the values of σ and ϕ at the horizon. The asymptotic expansion for the functions at infinity are given by

$$m(r) = M + \tilde{m}_1\frac{\exp(-2m_{\text{eff}}r)}{r} + \cdots, \tag{17}$$

$$\sigma(r) = \tilde{\sigma}_1\frac{\exp(-2m_{\text{eff}}r)}{r} + \cdots, \tag{18}$$

$$\phi(r) = \tilde{\phi}_{H,1}\frac{\exp(-m_{\text{eff}}r)}{r} + \cdots, \tag{19}$$

$$U(r) = U_\infty - \frac{Q}{r} + \cdots, \tag{20}$$

where $\tilde{m}_1$, $\tilde{\sigma}_1$, and $\tilde{\phi}_{H,1}$ are constants; U_∞ is the electric potential; and M is the ADM mass of the charged hairy black holes. Note that the denominator of $\phi_{H,1}$ has to be imposed with the condition $1 - \beta r_H^2 V(\phi_H) - \frac{\beta Q^2}{2r_H^2} \neq 0$ in order to keep $\phi(r)$ and $\sigma(r)$ finite at the horizon. Moreover, the effective mass of the scalar field is given by $m_{\text{eff}} = \sqrt{V_0\phi_0\phi_1}$.

Since the ODEs are nonlinear, it would be very challenging to obtain the closed form for the charged hairy black holes, although the ODEs look very simple, so we integrate the ODEs by the professional solver Colsys which employs the Newton-Raphson method to solve a set of nonlinear ODEs by providing the adaptive mesh refinement to generate the solutions with high accuracy and the estimation of errors of solutions [55]. In the numerics we compactify the radial coordinate r by $r = r_H/(1-x)$ with $x \in [0, 1]$ which can map the one-to-one correspondence of horizon and infinity to 0 and 1, respectively. We also introduce the following dimensionless parameters:

$$r \to \frac{r}{\sqrt{\beta}}, \qquad m \to \frac{m}{\sqrt{\beta}}, \qquad \phi \to \sqrt{\beta}\phi,$$
$$\phi_1 \to \sqrt{\beta}\phi_1, \qquad \phi_0 \to \sqrt{\beta}\phi_0, \qquad V \to \sqrt{\beta}V. \tag{21}$$

Therefore, we are left with the following free parameters: ϕ_0, ϕ_1, r_H, q, σ_H, ϕ_H, $\tilde{m}_1$, $\tilde{\sigma}_1$, $\tilde{\phi}_{H,1}$, U_∞, and M. The parameters σ_H, $\tilde{m}_1$, $\tilde{\sigma}_1$, $\tilde{\phi}_{H,1}$, U_∞, and M are determined when the solutions satisfy the boundary conditions; thus the input parameters in the numerics are given by ϕ_0, ϕ_1, r_H, q, and ϕ_H.

C. Basic properties of charged hairy black holes

In this subsection, we study the basic properties of charged hairy black holes; in particular, we are interested in the area of horizon A_H and Hawking temperature T_H of black holes,

$$A_H = 4\pi r_H^2, \qquad T_H = \frac{1}{4\pi} N'(r_H) e^{-\sigma_H}, \tag{22}$$

where σ_H is the value of function σ at the horizon. For the convenience of comparing our black hole solution with a known solution, which is the RNBH in this case, we introduce the following reduced quantities at the horizon of the black holes,

$$a_H = \frac{A_H}{16\pi M^2}, \qquad t_H = 8\pi T_H M. \tag{23}$$

The explicit form of a_H and t_H for the RNBH are given by [18]

$$a_H = \frac{1}{4}\left(1 + \sqrt{1-q^2}\right)^2, \quad t_H = \frac{4\sqrt{1-q^2}}{\left(1+\sqrt{1-q^2}\right)^2}, \tag{24}$$

where q is interpreted as ratio of the charge Q to the ADM mass M and defined as

$$q = \frac{Q}{M}. \tag{25}$$

The values of a_H and t_H are unity when the black hole is the Schwarzchild black hole ($q = 0$). a_H is bounded in between $1/4 \leq a_H \leq 1$ for the RNBH where $a_H = 1/4$ corresponds to the extremal RNBH ($q = 1$). Moreover, t_H is bounded in between $0 \leq t_H \leq 1$ for the RNBH where $t_H = 0$ corresponds to the extremal RNBH.

On the other hand, we could inspect the violation of the weak energy condition (WEC) for the hairy RNBHs since $V(\phi)$ is not entirely positive definite with $V(\phi) < 0$ in some regions of ϕ; thus the expression of WEC is given by

$$\rho = -T_t^t = \frac{N}{2}\phi'^2 + V + \frac{Q^2}{2r^4}. \tag{26}$$

We observe that ρ approaches zero at the infinity but at the horizon, given that $N(r_H) = 0$, the WEC of neutral hairy RNBHs which is from our previous work [35] is violated at the horizon with $\rho = V(\phi_H) < 0$. Therefore, it will be interesting to study if the inclusion of Q could reduce the violation of WEC.

D. The spherical perturbation

Here we study the linear stability of hairy black holes by performing the spherical perturbation on the background metric, scalar field, and the Maxwell field, respectively:

$$ds^2 = -N(r)e^{-2\sigma(r)}[1 + \epsilon e^{-i\omega t}F_t(r)]dt^2 + \frac{1}{N(r)}[1 + \epsilon e^{-i\omega t}F_r(r)]dr^2 + r^2(d\theta^2 + \sin^2\theta d\varphi^2), \tag{27}$$

$$\Phi = \phi(r) + \epsilon\Phi_1(r)e^{-i\omega t}, \tag{28}$$

$$\bar{U} = U(r) + \epsilon U_1(r)e^{-i\omega t}, \tag{29}$$

where $F_t(r)$, $F_r(r)$, $\Phi_1(r)$, and $U_1(r)$ are the small perturbations to the nonperturbed solutions. The substitution of the above Ansatz into Eqs. (3), (4), and (5) yields a set of ODEs for the perturbation functions to the first order of ϵ,

$$F_r = \beta r \Phi_1 \phi', \tag{30}$$

$$F_t' = -F_r' + 2\beta r \Phi_1' \phi', \tag{31}$$

$$U_1' = \frac{Q(F_t + F_r)e^{-\sigma}}{2r^2}, \tag{32}$$

$$\Phi_1'' = \left(\sigma' - \frac{N'}{N} - \frac{2}{r}\right)\Phi_1' + \left(\frac{1}{N}\frac{\partial^2 V}{\partial\phi^2} - \omega^2\frac{e^{2\sigma}}{N^2}\right)\Phi_1 + \frac{F_r}{N}\frac{\partial V}{\partial\phi} + \frac{F_r' - F_t'}{2}\phi'. \tag{33}$$

Equation (33) can be simplified using Eqs. (30) and (31). Then Eq. (33) can be transformed into a Schrödinger-like master equation by defining $Z(r) = r\Phi_1(r)$,

$$\frac{d^2 Z}{dr_*^2} + (\omega^2 - V_R(r))Z = 0, \tag{34}$$

with the effective potential $V_R(r)$,

$$V_R(r) = Ne^{-2\sigma}\left[-\frac{N}{r^2} + \frac{1}{2r^4}(\beta r^2 \phi'^2 - 1)(2\beta r^4 V - 2r^2 + \beta Q^2) + 2\beta r\phi' \frac{\partial V}{\partial \phi} + \frac{\partial^2 V}{\partial \phi^2}\right]. \tag{35}$$

The tortoise coordinate r_* is

$$\frac{dr_*}{dr} = \frac{e^\sigma}{N}. \tag{36}$$

If the mode $\omega^2 < 0$, this indicates that the perturbation Z is unstable where Z can grow exponentially with time. Nevertheless, the perturbation Z can be stable and decay exponentially with time when $\omega^2 > 0$. Since Eq. (34) is an eigenvalue problem, then we compute the mode numerically by using COLSYS and treating ω^2 as the eigenvalue. In the numerics, we demand that the first-order derivative of the perturbation function vanishes at the boundaries $\partial_r Z(r_H) = \partial_r Z(\infty) = 0$. Since Eq. (34) is homogeneous, we can introduce an auxiliary equation $\frac{d}{dr}\omega^2 = 0$, that allows us to impose the condition $Z(r_p) = 1$ at some point r_p which typically lies in the middle of horizon and infinity, in order to obtain a nontrivial and normalizable solution for Z. The eigenvalue ω^2 is found automatically when Z satisfies all the asymptotic boundary conditions.

III. RESULTS AND DISCUSSIONS

Recall that the input parameters in the calculation are given by ϕ_0, ϕ_1, r_H, q, and ϕ_H. To generate the solutions of charged hairy black holes, we choose the values of global minimum ϕ_1 as $\phi_1 = 0.5$, 1.0. For each ϕ_1, we fix several values for the electrical charge q in the range [0, 1] and then increase the scalar field at the horizon ϕ_H from $\phi_H = 0$ until $\phi_H = \phi_1$; hence we find that a family of charged hairy black holes bifurcates from the RNBH when ϕ_H is nontrivial. Here we identify the charged hairy black holes as the hairy RNBHs where the nonextremal case corresponds to $0 \leq q < 1$ and the extremal case corresponds to $q = 1$. Subsequently, we present their properties based on our numerical results.

First, we exhibit the reduced area of horizon a_H for the hairy RNBHs in Fig. 2 with (a) $\phi_1 = 0.5$ and (b) $\phi_1 = 1.0$. When $\phi_H = 0$, the charged black hole is merely the RNBH, and a_H is bounded in between [0.25, 1] (blue curve) where $a_H = 0.25$ corresponds to the extremal RNBH ($q = 1$) and $a_H = 1$ corresponds to the Schwarzschild black hole ($q = 0$). When $q = 0$, a branch of neutral hairy black holes (black curve) bifurcates from the Schwarzschild black hole when ϕ_H increases from $\phi_H = 0$ to $\phi_H = \phi_1$ where their properties have been studied extensively by the authors in [35]. In the case $q > 0$, when ϕ_H increases from $\phi_H = 0$ until $\phi_H = \phi_1$, a family of hairy RNBHs bifurcates from the RNBH where hairy RNBHs behave very differently than the RNBH, we find that a_H decreases monotonically from unity to zero. In the limit $\phi_H = \phi_1$, ϕ_H sits exactly at the global minimum of $V(\phi)$; hence hairy RNBHs do not exist anymore. Overall, a_H for both cases $\phi_1 = 0.5$ and $\phi_1 = 1.0$ behave qualitatively the same. Note that for a fixed value of ϕ_H, a_H decreases with the increase of q, which implies the ADM mass of hairy RNBHs increases when q increases; thus the extremal hairy RNBHs (red curve) are the most massive hairy black holes while the neutral hairy black holes (black curve) are the lightest hairy black holes. Moreover, the value of q in our theory is

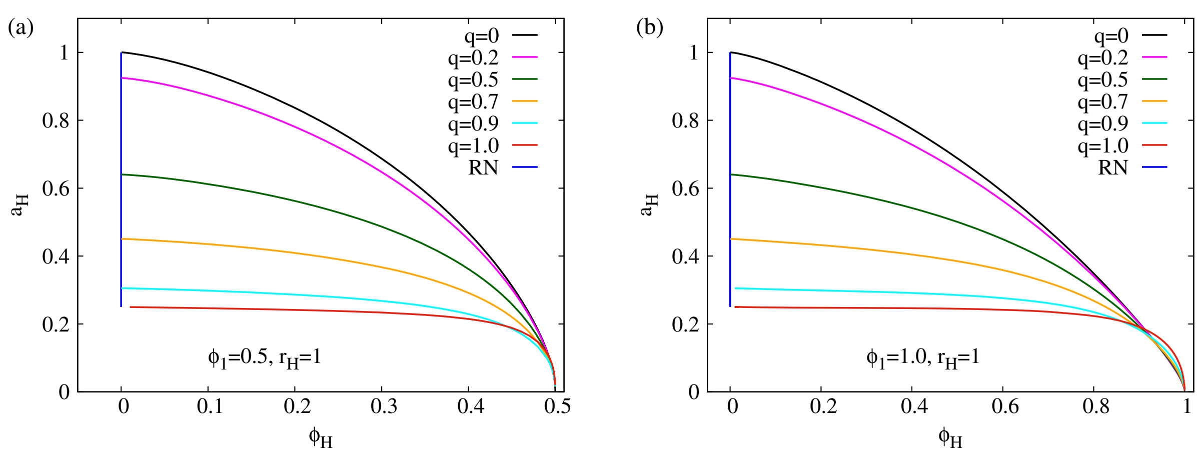

FIG. 2. The reduced area of horizon a_H of the hairy RNBHs with $r_H = 1$ and several q for (a) $\phi_1 = 0.5$ and (b) $\phi_1 = 1.0$.

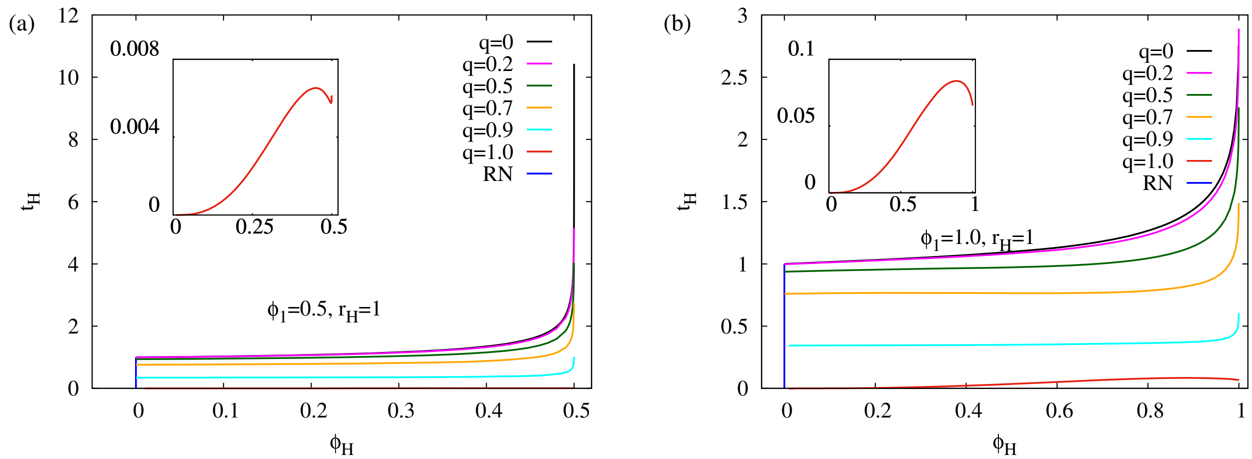

FIG. 3. The reduced Hawking temperature t_H of the hairy RNBHs with $r_H = 1$ and several q for (a) $\phi_1 = 0.5$ and (b) $\phi_1 = 1.0$.

bounded for $0 \leq q \leq 1$, where this is in contrast to the charged hairy black holes in the Einstein-Maxwell-scalar case where they can possess q greater than 1 [18,28]; thus our hairy RNBHs are not overcharged.

Second, we show the reduced Hawking temperature t_H for the hairy RNBHs in Fig. 3 with (a) $\phi_1 = 0.5$ and (b) $\phi_1 = 1.0$ analogous to a_H, when $\phi_H = 0$, t_H (blue curve) is bounded in $0 \leq t_H \leq 1$ where $t_H = 1$ corresponds to the Schwarzcshild black hole ($q = 0$) and $t_H = 0$ corresponds to the extremal Reissner-Nordström black hole ($q = 1$). Similarly, when ϕ_H increases, a branch of hairy RNBHs emerges from the RNBH for a fixed value of q. When $q = 0$, the corresponding hairy RNBHs are neutral where they have been considered by the authors in Ref. [35]. When $0 < q < 1$, t_H increases very sharply when ϕ_H increases from $\phi_H = 0$ to $\phi_H = \phi_1$; this also indicates that the hairy RNBHs do not exist when $\phi_H = \phi_1$. Interestingly, the inset of Figs. 3(a) and 3(b) demonstrates that t_H possesses a nonzero value when $q = 1$ where the extremal hairy RNBH emerges from the extremal RNBH. Furthermore, t_H behaves qualitatively the same for both cases $\phi_1 = 0.5$ and $\phi_1 = 1.0$.

Figure 4 exhibits the profiles of mass function $m(x)$ of the hairy RNBHs with $r_H = 1$ and $\phi_1 = 1.0$ in the compactified coordinate x for (a) $\phi_H = 0.5$ and (b) $\phi_H = 0.99$ (in the limit $\phi_H \to \phi_1$). We observe that $m(x)$ (black curve) with $q = 0$ as depicted in Figs. 4(a) and 4(b) possess almost a constant function inside the bulk, corresponding to the global minimum of the potential $V(\phi)$ which is the true vacuum ϕ_1. Moving away from the horizon, they develop a sharp boundary which looks like a global minimum at some intermediate region of the spacetime, where the functions rapidly change to another set of almost constant function which corresponds to the imposed false vacuum ($\phi = 0$) at infinity, where the scalar field sits in the local minimum. However, when q increases as shown in Fig. 4(a) for $\phi_H = 0.5$, the gradient of $m(x)$ at the horizon and the infinity also increases; thus $m(x)$ no longer possess almost constant functions inside the bulk and at the infinity; this has reduced the sharp boundary in

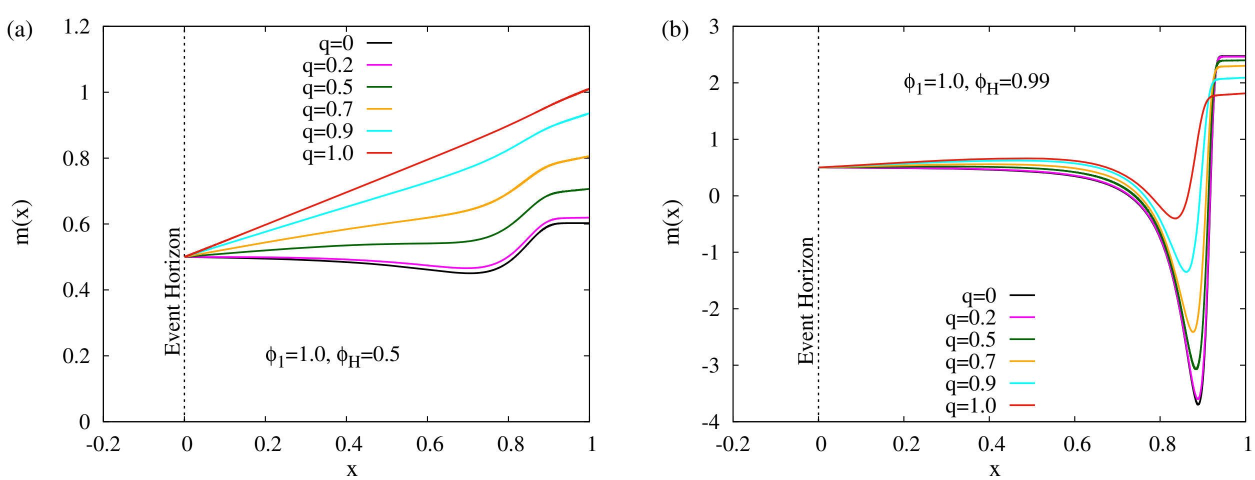

FIG. 4. The profiles of mass function $m(x)$ in the compactified coordinate x for the hairy RNBHs with $r_H = 1$, $\phi_1 = 1.0$, and several q for (a) $\phi_H = 0.5$ and (b) $\phi_H = 0.99$.

some intermediate region of the spacetime, as the consequence the global minimum is being lifted and then finally disappears. Thus, $m(x)$ (red curve) becomes almost a linear function when $q = 1$ for extremal hairy RNBHs. Nevertheless, Fig. 4(b) demonstrates that when $\phi_H = 0.99$, $m(x)$ still possess a sharp boundary that connects two different sets of almost constant functions at the horizon and the infinity, although that sharp boundary has been reduced with the increasing of q; therefore the global minimum of $m(x)$ still can exist even for $q = 1$ (red curve). Meanwhile, we find trivially that the profiles of solutions are heavily dominated by either the strength of q or ϕ_H.

Fig. 5 exhibits the profiles of scalar field $\phi(x)$ of the hairy RNBHs with $r_H = 1$ and $\phi_1 = 1.0$ in the compactified coordinate x for (a) $\phi_H = 0.1$ and (b) $\phi_H = 0.99$ (in the limit $\phi_H \to \phi_1$). Overall $\phi(x)$ decreases monotonically to zero from the horizon to the infinity. As shown in Fig. 5(a), when $\phi_H = 0.1$, the behavior of $\phi(x)$ is qualitatively similar to $m(x)$ where initially the gradient of $\phi(x)$ is very small for small q, but it becomes the steepest at the horizon when $q = 1$. This phenomenon can be described by the denominator of $\phi_{H,1}$ [Eq. (16)] where $V(\phi_H) < 0$ and $\frac{dV(\phi_H)}{d\phi} < 0$; the increasing of q decreases the denominator of $\phi_{H,1}$. Hence $\phi_{H,1}$ increases and then becomes largest but still remains finite when $q = 1$. Nevertheless, when we increase ϕ_H, for instance, $\phi_H = 0.99$ as shown in Fig. 5(b), the increasing of ϕ_H can flatten the profile of the scalar field in the bulk because the increasing of $V(\phi_H)$ increases the denominator of $\phi_{H,1}$; hence $\phi(x)$ looks like an almost constant function and is unaffected by q in the bulk.

Figure 6 exhibits the profiles of metric function $\sigma(x)$ of the hairy RNBHs with $r_H = 1$ and $\phi_1 = 1.0$ in the compactified coordinate x for (a) $\phi_H = 0.5$ and (b) $\phi_H = 0.99$ (in the limit $\phi_H \to \phi_1$). In general $\sigma(x)$ behaves quite similarly to the function $\phi(x)$ where it also

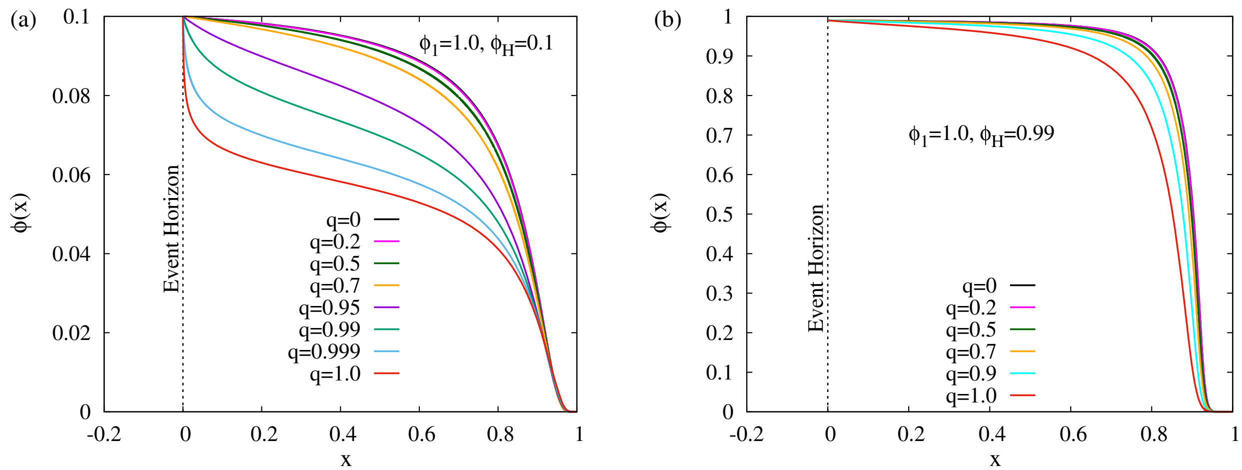

FIG. 5. The profiles of scalar field $\phi(x)$ in the compactified coordinate x for the hairy RNBHs with $r_H = 1$, $\phi_1 = 1.0$, and several q for (a) $\phi_H = 0.1$ [56] and (b) $\phi_H = 0.99$.

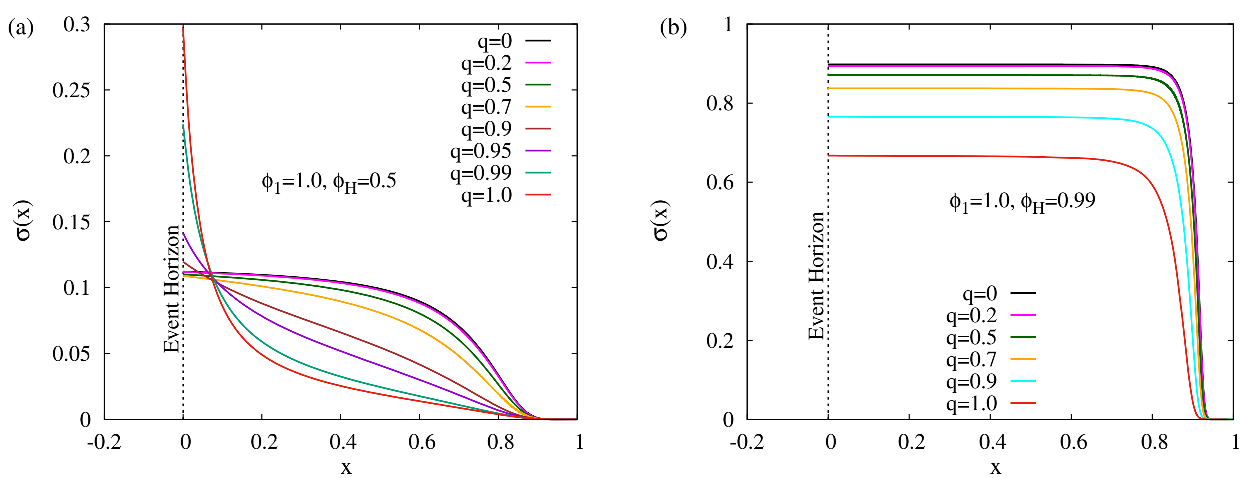

FIG. 6. The profiles of metric function $\sigma(x)$ in the compactified coordinate x for the hairy RNBHs with $r_H = 1$, $\phi_1 = 1.0$, and several q for (a) $\phi_H = 0.5$ and (b) $\phi_H = 0.99$.

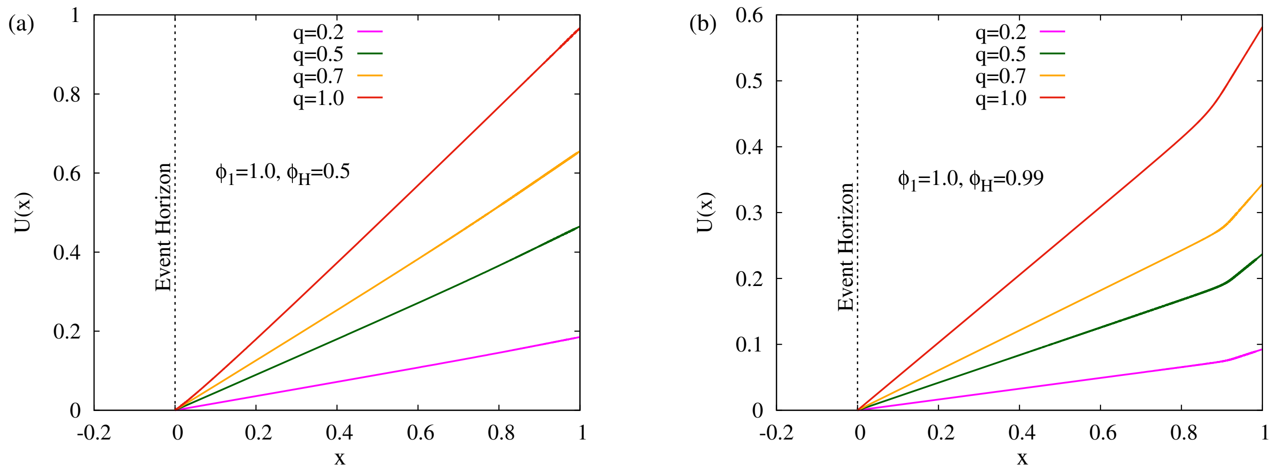

FIG. 7. The profiles of gauge field $U(x)$ in the compactified coordinate x for the hairy RNBHs with $r_H = 1$, $\phi_1 = 1.0$, and several q for (a) $\phi_H = 0.5$ and (b) $\phi_H = 0.99$.

decreases monotonically to zero from the horizon to the infinity. As shown in Fig. 6(a) for $\phi_H = 0.1$, the profile of $\sigma(x)$ is analogous to $\phi(x)$ for small q where the gradient of $\sigma(x)$ is very small which also looks like almost a constant function at the horizon that corresponds to the true vacuum ϕ_1. However, the value of $\sigma(x)$ and its gradient at the horizon increase very sharply when q increases where it follows the similar changes of $\phi(x)$ since $\sigma_1 \propto \phi_{H,1}^2$ [see Eq. (16)]. Hence, $\sigma(x)$ (red curve) is the steepest at the horizon when $q = 1$. However, when ϕ_H is large, for instance as demonstrated in Fig. 6(b), the gradient of $\sigma(x)$ at the horizon is unaffected by any values of q since $\phi_{H,1}$ is very small; thus we observe that $\sigma(x)$ still can behave like an almost constant function in the bulk.

Figure 7 shows the profiles of gauge field $U(x)$ of the hairy RNBHs with $r_H = 1$ and $\phi_1 = 1.0$ in the compactified coordinate x for (a) $\phi_H = 0.5$ and (b) $\phi_H = 0.99$. In Fig. 7(a), the profile of $U(x)$ is a linear function, and its gradient increases with the increase of q. In Fig. 7(b), $U(x)$ is still a linear function that increases linearly with the increase of x but increases a little sharply with a larger gradient near $x = 1$.

Figure 8 shows the WEC of Eq. (26) with several values of q in the compactified coordinate x for (a) $\phi_H = 0.5$ and $\phi_H = 0.99$. When $\phi_H = 0.5$ and $q = 0$, we observe that the WEC is violated since the local energy density is negative ($\rho = V(\phi_H) < 0$), particularly at the horizon. When we increase q, ρ can become strictly positive since the inclusion of q can reduce the violation of WEC. Hence, it gives us an important hint that the WEC of neutral hairy black holes in Ref. [36] can be possibly satisfied if they become charged black holes. When $\phi_H = 1.0$ and $q = 0$, WEC is violated at the horizon since $\rho < 0$. Similarly, WEC is also being satisfied at the horizon when we increase q. However, WEC is slightly violated in some regimes of x since $\rho < 0$. Note that there are some small

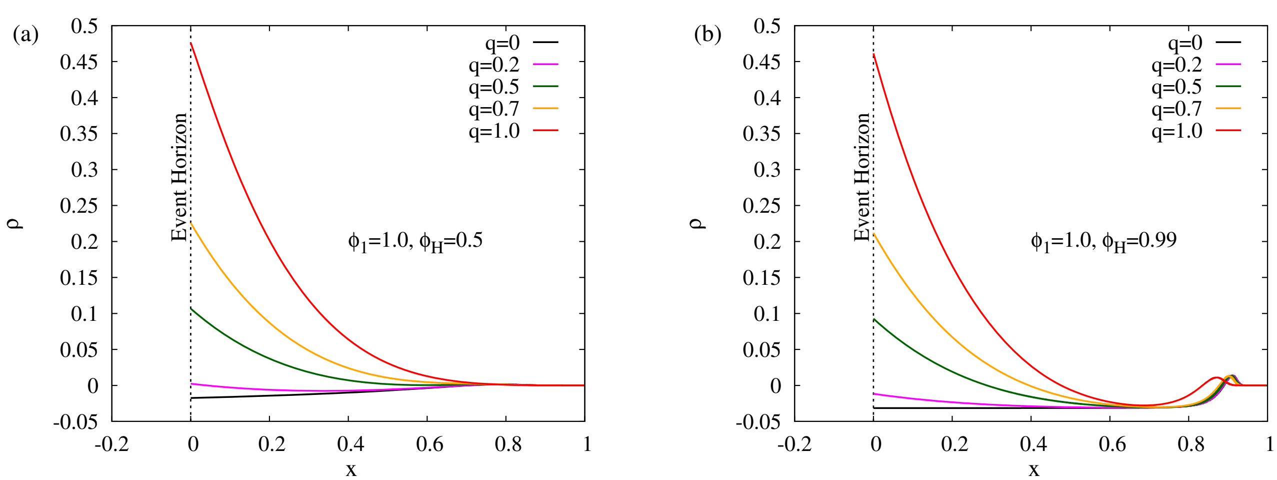

FIG. 8. The weak energy condition ρ in the compactified coordinate x for the hairy RNBHs with $r_H = 1$, $\phi_1 = 1.0$, and several q for (a) $\phi_H = 0.5$ and (b) $\phi_H = 0.99$.

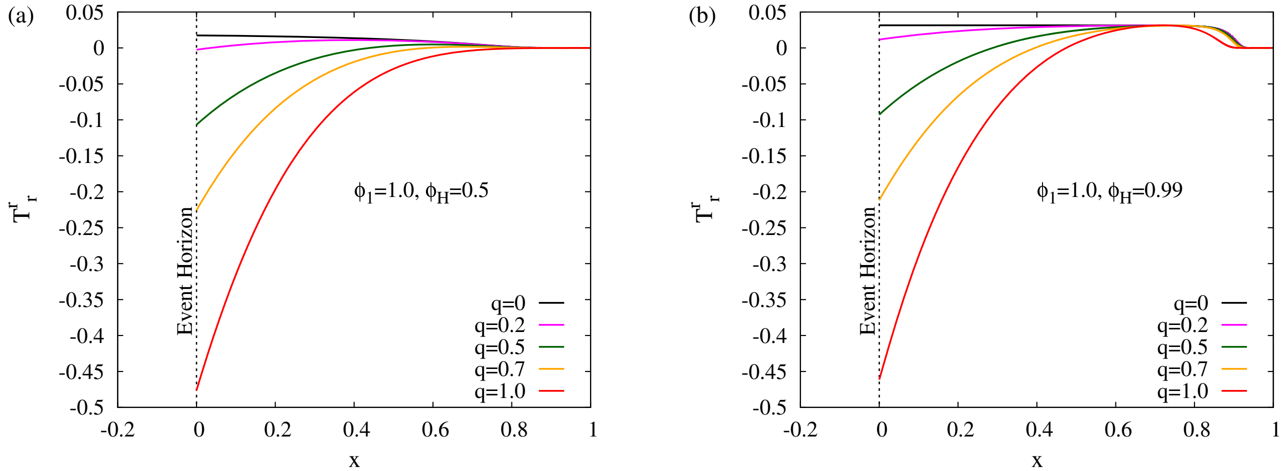

FIG. 9. The energy condition $T^r{}_r$ in the compactified coordinate x for the hairy RNBHs with $r_H = 1$, $\phi_1 = 1.0$, and several q for (a) $\phi_H = 0.5$ and (b) $\phi_1 = 0.99$.

peaks that form near $x = 1$ due to the global minimum of $m(x)$.

Meanwhile, the quantity T^r_r is depicted in Fig. 9 for a) $\phi_H = 0.5$ and b) $\phi_H = 0.99$. According to the no-hair theorem, T^r_r has to be negative and decreasing with r near the horizon [1,57]. When $\phi_H = 0.5$ and $q = 0$, the energy condition of T^r_r is violated at the horizon since $T^r_r > 0$, although it decreases monotonically after the horizon. However, when we increase q and find that $T^r_r < 0$, particularly at the horizon, but it increases with x near the horizon, the criteria for T^r_r set by the no-hair theorem is still being violated. Similarly, when $\phi_H = 0.99$ and $q = 0$, the energy condition of T^r_r is being violated since it is strictly positive, although it decreases monotonically. Nevertheless, when we increase q, although we find that $T^r_r < 0$, particularly at the horizon, the criteria for T^r_r is still violated since it increases monotonically. Analogous to ρ, T^r_r possesses a local maximum exactly at the location of the global minimum of $m(x)$.

Figure 10 shows the parameter ϕ_0 as the function of ϕ_H for $\phi_1 = 0.5$ and $\phi_1 = 1.0$. Both cases $(\phi_1 = 0.5, 1.0)$ demonstrate that ϕ_0 increases monotonically as ϕ_H increases from zero, and ϕ_0 is almost indistinguishable for small q but becomes distinct when $q \to 1$.

Figure 11 shows the profiles of the potential $V(\phi)$ for (a) $\phi_1 = 0.5$, $q = 0.5$ and (b) $\phi_1 = 1.0$, $q = 0.5$. $V(\phi)$ contains three roots, and the negative region of $V(\phi)$ is bounded by two roots. When ϕ_H increases, we find that the global minimum $V(\phi_1)$ has been lifted while ϕ_0 moves toward ϕ_1, and the height of barrier $V(\phi_0)$ increases as well. Note that the values of $V(\phi_H)$ are always negative.

Figures 12(a) and 12(b) exhibit the effective potential $V_R(x)$ in the compactified coordinate x for $\phi_1 = 1.0$. We observe that some region of $V_R(x)$ is negative; this indicates the instability might appear in the configuration of hairy RNBH. Thus, we can show the existence of the unstable modes ω^2 for the black hole configuration with $\phi_1 = 0.5$ and $\phi_1 = 1.0$ in Figs. 13(a) and 13(b),

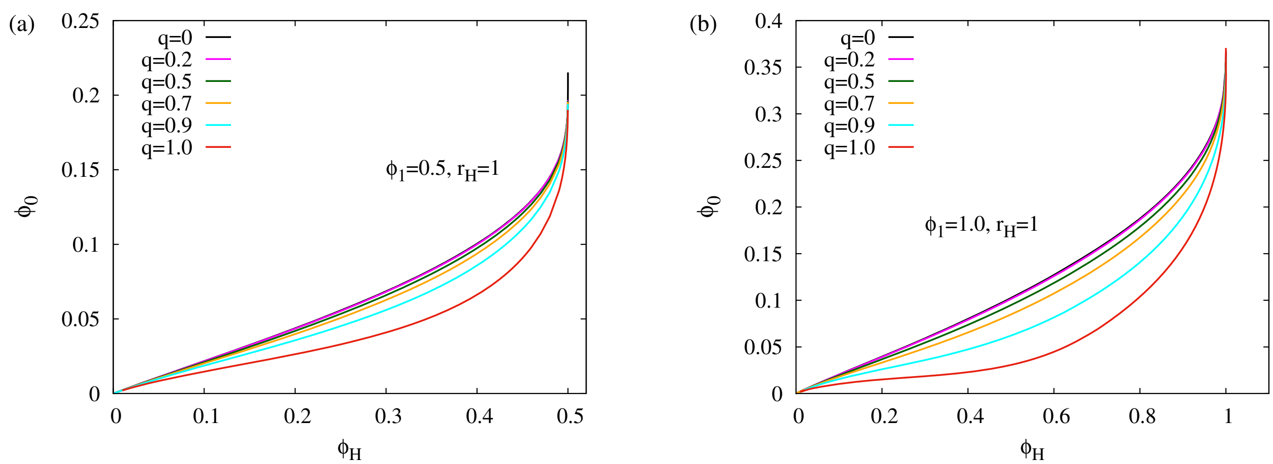

FIG. 10. The parameter ϕ_0 as the function of ϕ_H for the hairy RNBHs with $r_H = 1$ and several q for (a) $\phi_1 = 0.5$ and (b) $\phi_1 = 1.0$.

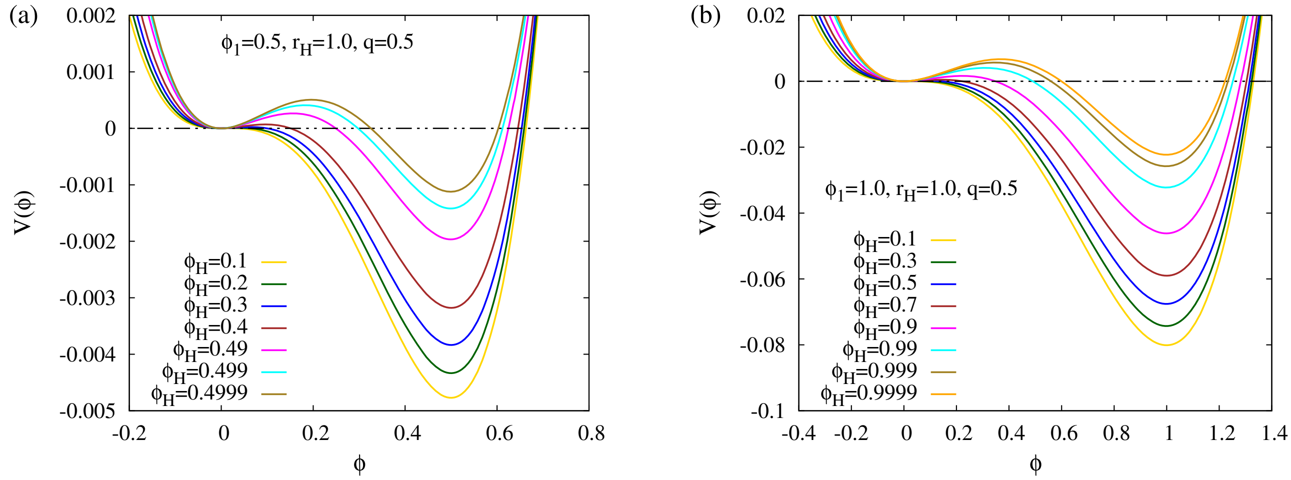

FIG. 11. The profiles of the potential $V(\phi)$ with several ϕ_H for (a) $\phi_1 = 0.5$, $q = 0.5$; (b) $\phi_1 = 1.0$, $q = 0.5$.

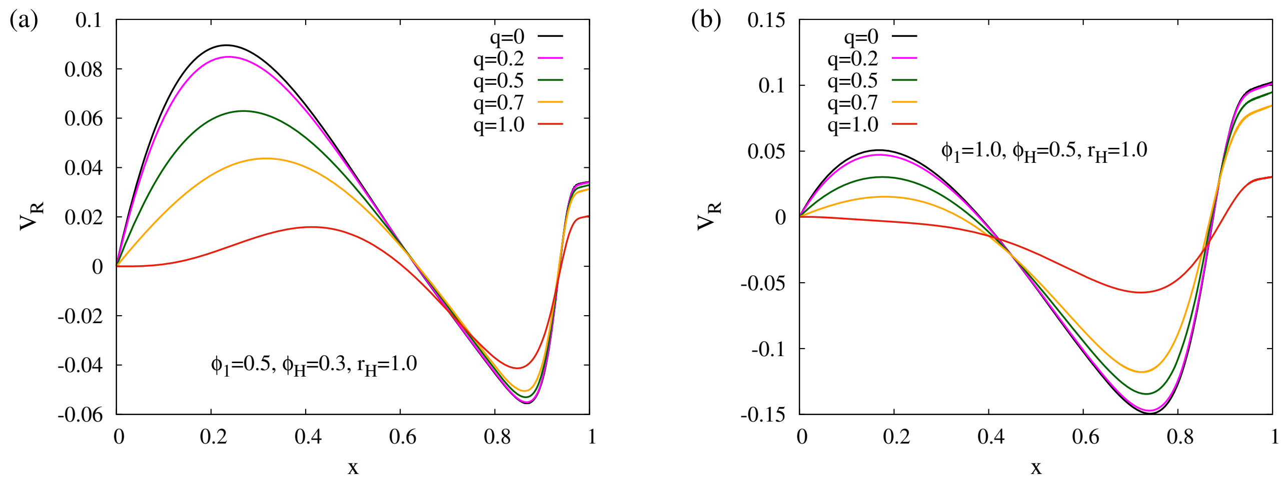

FIG. 12. The effective potential V_R in the compactified coordinate x for the hairy RNBHs with $r_H = 1$ and several q for (a) $\phi_1 = 0.5$, $\phi_H = 0.3$ and (b) $\phi_1 = 1.0$, $\phi_H = 0.5$.

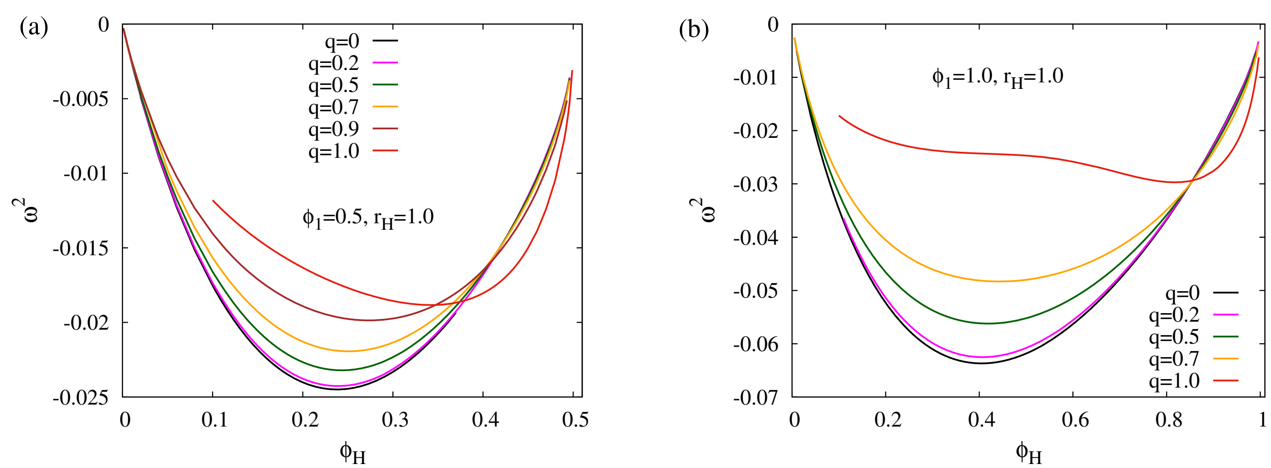

FIG. 13. The unstable modes of hairy RNBHs with $r_H = 1$ and several q for (a) $\phi_1 = 0.5$ and (b) $\phi_1 = 1.0$.

respectively by numerically solving Eq. (34). For a fixed q, as ϕ_H increases from zero, we observe that ω^2 decreases from zero to a minimum value, and then increases again to approach zero in the limit $\phi_H \to \phi_1$. The existence of unstable modes implies the hairy RNBH are unstable and the perturbation will grow exponentially with time. The unstable modes only disappear in the limit $\phi_H \to \phi_1$ where the hairy RNBHs do not exist anymore in that limit. Note that ω^2 increases with the increasing of q for a fixed ϕ_H with a certain range; this implies the q could "weakly" improve the stability of the hairy RNBHs. Hence, the extremal hairy RNBH is relatively more stable than other nonextremal hairy RNBH for a certain range of ϕ_H.

IV. CONCLUSION

In this paper, we have broadened the class of RNBH by minimally coupling a scalar potential $V(\phi)$ in the EMKG theory to construct charged hairy black holes. Here we introduce $V(\phi)$ which possesses a local minimum, a global minimum ϕ_1, and a local maximum ϕ_0 where it has been applied in the cosmology to describe the phase transition of bubbles from the false vacuum (local maximum) to the true vacuum (global minimum). Previously the corresponding $V(\phi)$ has been applied by the authors to construct the asymptotically flat neutral hairy black holes [35], and hence, we generalize them to the charged hairy black holes which possess the electric charge Q.

In the EMKG theory, the trivial solution is the RNBH with the scalar field diverging at the horizon when $V(\phi)$ does not exist. When we include $V(\phi)$, we demonstrate that it is possible to circumvent the no-hair theorem where we can obtain the charged hairy black holes that are globally regular outside the horizon. Thus, the family of hairy charged black holes emerges from the RNBH with a fixed value of charge per unit mass, $q = Q/M$ when the scalar field at the horizon ϕ_H is nontrivial and we can identify the charged hairy black holes as the hairy RNBHs. The value of q is bounded in [0, 1] where $q = 0$ corresponds to the neutral hairy black holes [35] and $0 \leq q < 1$ corresponds to nonextremal hairy RNBHs, while $q = 1$ corresponds to the extremal hairy RNBHs. This is also in contrast to the hairy black holes in the Einstein-Maxwell-scalar theory where they can possess $q > 1$ [18,28].

The properties of neutral hairy black holes ($q = 0$) have been studied previously by the authors [35]. Here we study the properties of hairy RNBHs by choosing $\phi_1 = 0.5$, 1.0, and then we fix a value of q; when we increase ϕ_H from zero, we find that the reduced area of horizon a_H decreases from unity to zero while the reduced Hawking temperature t_H increases very sharply when $\phi_H = \phi_1$. This might imply that the hairy RNBHs do not exist in that limit. Note that the extremal hairy RNBHs possess the nontrivial t_H while RNBH possesses the vanishing t_H.

Then we briefly summarize the profiles of solutions. When $q = 0$, the mass function possesses almost a constant function inside the bulk, corresponding to the global minimum of the potential $V(\phi)$ which is the true vacuum ϕ_1. Moving away from the horizon, it develops a sharp boundary which looks like a global minimum at some intermediate region of the spacetime, where the function rapidly changes to another set of almost constant function which corresponds to the imposed false vacuum ($a = 0$) at infinity, where the scalar field sits in the local minimum. When $\phi_H = 0.5$ with $q \neq 0$, the gradient of mass function at the horizon and the infinity increases; hence the sharp boundary is reduced, and then the global minimum is being lifted when we increase q. Thus the global minimum disappears for the extremal case ($q = 1$), and the mass function looks like a linear function as a consequence. When $\phi_H = 0.99$, the two different sets of almost constant functions are still connected by a sharp boundary although the global minimum is also being lifted slightly but eventually still can be preserved when $q = 1$. The scalar field decreases monotonically from its maximum value at the horizon to zero at the infinity. When $\phi_H = 0.1$, the scalar field also possesses an almost constant function at the horizon, but its gradient at the horizon increases very sharply when q increases; thus it is the steepest at the horizon when $q = 1$. However, the gradient of the scalar field at the horizon can still become very small when $\phi_H = 0.99$, even $q = 1$. Furthermore, the gauge field increases linearly from the horizon to the infinity. When $\phi_H = 0.99$, the gradient of the gauge field slightly increases near the infinity for $\phi_1 = 1.0$. Overall, we find a very interesting phenomenon that the profiles of solutions are heavily dominated by either the electric charge q or the scalar field.

The WEC which can be described by the local energy density $\rho = -T^t{}_t$ is violated, particularly at the horizon for the neutral hairy RNBHs ($q = 0$). However, WEC can be satisfied with $\rho > 0$ at the horizon when $q \neq 0$ for $\phi_1 = 0.5$. Thus, this could imply that the WEC of neutral hairy black holes [36] can be possibly satisfied if they become charged black holes. Nevertheless, WEC is slightly violated in the region of compactified coordinate $0.5 < x < 1$ for $\phi_1 = 1.0$ although q increases. Meanwhile, the component of stress-energy tensor $T^r{}_r$ is strictly positive for neutral hairy black holes ($q = 0$) but becomes negative, particularly at the horizon when $q \neq 0$ for $\phi_1 = 0.5$, 1.0.

The neutral hairy black holes from our previous work [35] are found to be unstable against the linear perturbation. We also study the stability of hairy RNBHs by performing the spherical perturbation to the background spacetime and the matter fields to obtain the Schrödinger-like master equation. We perform the numerical mode analysis and then find that the solutions of the hairy RNBHs also possess the unstable modes; hence they are also unstable against the linear perturbation. Here we find that the presence of q merely "weakly" improves the stability of the hairy RNBHs where the extremal hairy

RNBHs could be relatively stable than nonextremal hairy RNBHs for a certain range of ϕ_H. Note that the unstable modes only disappear when $\phi_H \to \phi_1$ where the hairy RNBHs do not exist anymore in that limit.

There also could be several extensions from this work. First, we can consider the dyon case where the hairy RNBHs can possess the magnetic charge and study their properties systematically. Then, it will be worthwhile to stress that the hairy RNBHs recently have gained some interest in the context of the Cauchy horizon theorems where some research shows that the inner Cauchy horizon may not exist if there is a scalar hair at the outer horizon [58–62]. Hence, the investigation of the dynamical evolution of charged hairy black holes will be useful for us to understand the process of formation of the Cauchy horizon, since we lack the analytical proof on this [50].

Therefore, we can study the nonexistence of the Cauchy horizon for the hairy RNBHs by following the approaches from Refs. [47,48] to adopt a static metric with spherical and planar symmetries, which can describe the interior of the hairy RNBHs by solving the equations of motion numerically. We can also adopt the double-null formalism to study the evolution of hairy RNBHs by employing a generic metric in the double-null coordinate,

$$ds^2 = -\alpha^2(u,v)dudv + r^2(u,v)(d\theta^2 + \sin^2\theta d\varphi^2), \quad (37)$$

where u and v denote the ingoing null direction and outgoing null direction, respectively. Then Eq. (37) can be substituted into the EMKG system to obtain a set of nonlinear partial differential equations with respect to u and v, which can be solved numerically with appropriate boundary conditions. However, our solutions only cover from the horizon to the infinity; hence we probably still need to obtain the interior solutions of hairy RNBHs which served as the initial condition for the numerics, so we will leave this as a future investigation.

ACKNOWLEDGMENTS

X. Y. C. is supported by the starting grant of Jiangsu University of Science and Technology (JUST). D. Y. is supported by the National Research Foundation of Korea (Grants No. 2021R1C1C1008622 and No. 2021R1A4A5031460). X. Y. C. is grateful for the hospitality provided by the organizer of the conference “String, Gravity and Cosmology 2023” which was held in Busan, Korea.

[1] J. D. Bekenstein, Phys. Rev. D **51**, R6608 (1995).
[2] W. Israel, Phys. Rev. **164**, 1776 (1967).
[3] R. Ruffini and J. A. Wheeler, Phys. Today **24**, No. 1, 30 (1971).
[4] H. Reissner, Ann. Phys. (Berlin) **50**, 106 (1916).
[5] G. Nordstrom, Proc. Kon. Ned. Akad. Wet. **20**, 1238 (1918).
[6] G. W. Gibbons and K. i. Maeda, Nucl. Phys. **B298**, 741 (1988).
[7] D. Garfinkle, G. T. Horowitz, and A. Strominger, Phys. Rev. D **43**, 3140 (1991); **45**, 3888(E) (1992).
[8] P. Dobiasch and D. Maison, Gen. Relativ. Gravit. **14**, 231 (1982).
[9] G. W. Gibbons and D. L. Wiltshire, Ann. Phys. (N.Y.) **167**, 201 (1986); **176**, 393(E) (1987).
[10] R. Kallosh, A. D. Linde, T. Ortin, A. W. Peet, and A. Van Proeyen, Phys. Rev. D **46**, 5278 (1992).
[11] A. Anabalon, D. Astefanesei, and R. Mann, J. High Energy Phys. 10 (2013) 184.
[12] C. A. R. Herdeiro, E. Radu, N. Sanchis-Gual, and J. A. Font, Phys. Rev. Lett. **121**, 101102 (2018).
[13] P. G. S. Fernandes, C. A. R. Herdeiro, A. M. Pombo, E. Radu, and N. Sanchis-Gual, Classical Quantum Gravity **36**, 134002 (2019); **37**, 049501(E) (2020).
[14] Y. S. Myung and D. C. Zou, Eur. Phys. J. C **79**, 273 (2019).
[15] Y. S. Myung and D. C. Zou, Phys. Lett. B **790**, 400 (2019).
[16] Y. S. Myung and D. C. Zou, Eur. Phys. J. C **79**, 641 (2019).
[17] D. Astefanesei, D. Choque, F. Gómez, and R. Rojas, J. High Energy Phys. 03 (2019) 205.
[18] D. Astefanesei, C. Herdeiro, A. Pombo, and E. Radu, J. High Energy Phys. 10 (2019) 078.
[19] J. L. Blázquez-Salcedo, S. Kahlen, and J. Kunz, Eur. Phys. J. C **79**, 1021 (2019).
[20] D. Astefanesei, J. L. Blázquez-Salcedo, C. Herdeiro, E. Radu, and N. Sanchis-Gual, J. High Energy Phys. 07 (2020) 063.
[21] Y. S. Myung and D. C. Zou, Phys. Lett. B **811**, 135905 (2020).
[22] P. G. S. Fernandes, Phys. Dark Universe **30**, 100716 (2020).
[23] D. Astefanesei, J. Luis Blázquez-Salcedo, F. Gómez, and R. Rojas, J. High Energy Phys. 02 (2021) 233.
[24] J. Luis Blázquez-Salcedo, C. A. R. Herdeiro, S. Kahlen, J. Kunz, A. M. Pombo, and E. Radu, Eur. Phys. J. C **81**, 155 (2021).
[25] J. L. Blázquez-Salcedo, C. A. R. Herdeiro, J. Kunz, A. M. Pombo, and E. Radu, Phys. Lett. B **806**, 135493 (2020).
[26] M. Y. Lai, Y. S. Myung, R. H. Yue, and D. C. Zou, Phys. Rev. D **106**, 044045 (2022).
[27] Y. Liu, C. Y. Zhang, Q. Chen, Z. Cao, Y. Tian, and B. Wang, Sci. China Phys. Mech. Astron. **66**, 100412 (2023).
[28] S. Kiorpelidi, T. Karakasis, G. Koutsoumbas, and E. Papantonopoulos, Phys. Rev. D **109**, 024033 (2024).
[29] Z. Belkhadria and A. M. Pombo, Phys. Rev. D **110**, 044014 (2024).

[30] G. Guo, P. Wang, H. Wu, and H. Yang, J. High Energy Phys. 10 (2023) 076.
[31] W. Xiong, C. Y. Zhang, and P. C. Li, arXiv:2312.11879.
[32] Y. Meng, X. M. Kuang, X. J. Wang, B. Wang, and J. P. Wu, Eur. Phys. J. C **84**, 305 (2024).
[33] T. Damour and G. Esposito-Farese, Phys. Rev. Lett. **70**, 2220 (1993).
[34] A. Corichi, U. Nucamendi, and M. Salgado, Phys. Rev. D **73**, 084002 (2006).
[35] X. Y. Chew, D. h. Yeom, and J. L. Blázquez-Salcedo, Phys. Rev. D **108**, 044020 (2023).
[36] X. Y. Chew and K. G. Lim, Phys. Rev. D **109**, 064039 (2024).
[37] S. R. Coleman and F. De Luccia, Phys. Rev. D **21**, 3305 (1980).
[38] O. Bechmann and O. Lechtenfeld, Classical Quantum Gravity **12**, 1473 (1995).
[39] H. Dennhardt and O. Lechtenfeld, Int. J. Mod. Phys. A **13**, 741 (1998).
[40] K. A. Bronnikov and G. N. Shikin, Gravitation Cosmol. **8**, 107 (2002).
[41] C. Martinez, R. Troncoso, and J. Zanelli, Phys. Rev. D **70**, 084035 (2004).
[42] V. V. Nikonov, J. V. Tchemarina, and A. N. Tsirulev, Classical Quantum Gravity **25**, 138001 (2008).
[43] A. Anabalon and J. Oliva, Phys. Rev. D **86**, 107501 (2012).
[44] C. Lan, H. Yang, Y. Guo, and Y. G. Miao, Int. J. Theor. Phys. **62**, 202 (2023).
[45] W. K. Ahn, B. Gwak, B. H. Lee, and W. Lee, Eur. Phys. J. C **75**, 372 (2015).
[46] B. H. Lee, W. Lee, and D. Ro, Phys. Rev. D **99**, 024002 (2019).
[47] Y. S. An, L. Li, and F. G. Yang, Phys. Rev. D **104**, 024040 (2021).
[48] R. G. Cai, L. Li, and R. Q. Yang, J. High Energy Phys. 03 (2021) 263.
[49] D. O. Devecioglu and M. I. Park, Phys. Lett. B **829**, 137107 (2022).
[50] X. Y. Chew and D. h. Yeom, arXiv:2308.09225.
[51] Y. C. Ong, Eur. Phys. J. C **83**, 1068 (2023).
[52] X. Y. Chew and K. G. Lim, Universe **10**, 212 (2024).
[53] L. Del Grosso and P. Pani, Phys. Rev. D **108**, 064042 (2023).
[54] C. W. Misner and D. H. Sharp, Phys. Rev. **136**, B571 (1964).
[55] U. Ascher, J. Christiansen, and R. D. Russell, Math. Comput. **33**, 659 (1979).
[56] We initially wanted to set Fig. 5(a) as $\phi_H = 0.5$ but found that the scalar field at the horizon is not so steep if compared to the case $\phi_H = 0.1$ when $q \to 1$; hence we just set Fig. 5(a) as $\phi_H = 0.1$ which can obviously demonstrate that $\phi(x)$ can be very steep at the horizon.
[57] P. Dorlis, N. E. Mavromatos, and S. N. Vlachos, Phys. Rev. D **108**, 064004 (2023).
[58] J. Hansen and D. Yeom, J. High Energy Phys. 10 (2014) 040.
[59] J. Hansen and D. Yeom, J. Cosmol. Astropart. Phys. 09 (2015) 019.
[60] A. Nakonieczna and D. Yeom, J. High Energy Phys. 02 (2016) 049.
[61] A. Nakonieczna and D. Yeom, J. High Energy Phys. 05 (2016) 155.
[62] Y. Brihaye, C. Herdeiro, and E. Radu, Phys. Lett. B **760**, 279 (2016).